

## CHARGE TRANSFER BY $H^+$ ION IMPACT FROM H AND Na ATOMS ADSORBED ON Al(100) SURFACE\*

HIROYA SUNO

*Japan Agency for Marine-Earth Science and Technology (JAMSTEC),  
Yokohama, Japan*

REIKO SUZUKI

*Computer Center, Hitotsubashi University, Kunitachi, Tokyo, Japan*

DAIJI KATO

*National Institute for Fusion Science, Toki, Japan*

LUKAS PICHL

*International Christian University, Tokyo, Japan*

MINEO KIMURA\*\*

*Graduate School of Sciences, Kyushu University, Fukuoka, Japan*

### *Abstract*

Collision processes between the hydrogen ion  $H^+$  and an atom adsorbed on the Al(100) surface at grazing incident angles are investigated. A semiclassical close-coupling scheme is employed in order to calculate the probabilities for elastic scattering and charge transfer between the  $H^+$  ion and the hydrogen- or sodium-atom adsorbed Al(100) surface for incident kinetic energies between 10 eV and 10 keV. Charge transfer is found to take place significantly between the  $H^+$  ion and the hydrogen atom, while it is suppressed in the case of the sodium atom. We also study the orientation and alignment of the cloud of the electron captured in  $2p$  states by the  $H^+$  ion.

---

\* This work was supported in part by the Grant-in-Aid from the Ministry of Education, Science, Sport, Culture and Technology (HS, RS and MK), Japan-Germany Collaborative Research Program of Japan Society for Promotion of Science (HS and MK), and Cooperative Research Grant from National Institute for Fusion Science, Japan. We would like to thank Professor Robert J. Buenker at Bergische University, Dr. Chizuko Dutta and Professor Peter Nordlander at Rice University for giving us an opportunity of conducting this research together.

\*\* Deceased

## I. *Introduction*

Charge transfer by ions, atoms and molecules from a solid surface plays a crucial role in a number of important physical processes, and inclusive are the sticking, desorption, and dissociation. This also serves as a base for ion-beam electron-capture spectroscopy which is used as a powerful tool to investigate various properties of surfaces such as thermodynamic and critical behavior of surfaces, or magnetic and electronic characteristics not only from metals but also organic compounds. Recently, charge transfer shows a strong come-back as an urgent problem owing partly to the requirement of more high-resolution techniques from areas like plasma processing. It has been also a center of subject in astrochemistry where various molecules are known to form on the grain/surface of cluster in interstellar space.

Not only mentioning experimental efforts, there have been various theoretical attempts to study charge transfer from a surface, mostly, using the solution of the time-dependent Anderson model and its simplified version from surface scientists [1-4]. We can also mention the review paper by H. Winter, treating the collisions of atoms and ions with surfaces under grazing incidence [5]. Despite these intensive efforts, there is still considerable lack of understanding of charge transfer processes. To contribute toward better understanding, we feel that it is necessary to investigate the subject with a unified effort from atomic and molecular physics and surface physics.

In this paper, we investigate charge transfer from H or Na atom adsorbed on Al(100) surface by  $H^+$  ion impact from 10 eV to 10 keV. H, Na and Al atoms have the Pauling electron-affinity value of 2.1, 0.9 and 1.5, respectively, and hence, for the [H-Al(100)] system, the electron charge distribution is pulled toward the adsorbed H atom from the surface, while for the [Na-Al(100)] system, it is reversed. Upon impinging  $H^+$  ion on H or Na adsorbed surface, the incoming  $H^+$  ion sees completely different environment near the surface, and therefore, it is extremely interesting to carry out a detailed comparative study of charge transfer dynamics between these two systems to answer some questions like why and how charge transfer would occur or not occur and what is the spin state after charge transfer. In the present calculation, Al atoms which constitute the surface are explicitly considered up to 72 atoms, in addition to adsorbed H or Na atoms, in the calculation of electronic states of the whole system and a semiclassical treatment for scattering dynamics is employed. Inclusion of a large number of atoms for mimicking the surface property properly is the first trial of this kind, as far as we know, and should be expected to provide more realistic information about charge transfer.

The plan of this paper is as follows. In Sec. II, we explain our theoretical method to calculate the probabilities for elastic scattering and charge transfer. Our results are presented in Sec. III in the form of a comparison between the H-adsorbed and Na-adsorbed surfaces. A summary of this work is given in Sec. IV. We use atomic units throughout except where explicitly states otherwise.

## II. *Theoretical Model*

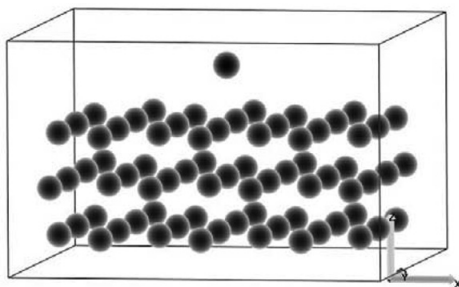
Our theoretical method consists of a combination of a self-consistent field (SCF) method and a semiclassical close-coupling scheme. SCF calculations are carried out in order to obtain

the electrostatic potential and the ground-state electronic wavefunction of the atom-adsorbed surface. The semiclassical close-coupling method is then used to calculate the probabilities for elastic scattering and charge transfer in collision between the H<sup>+</sup> ion and the surface.

## 1. Electronic States of Surface

The electrostatic potential of the atom-adsorbed surface is obtained from an SCF calculation using the GAUSSIAN 98 quantum chemistry software [6]. The obtained electrostatic potential  $V_e$  equals, with a minus sign (in atomic units), the interaction potential between the H<sup>+</sup> ion and the surface. Our Al(100) surface adsorbed by an atom X is modeled as a cluster of 73 atoms XAl<sub>72</sub>, including totally 72 Al atoms in 3 atomic layers and an additional X atom, as shown in Fig. 1. Our SCF calculations are carried out using Slater-Type Orbitals (STO-3G basis) approximated by 3 Gaussian functions for a charge state of +1 and a multiplicity of +2, with a spatial grid  $200 \times 200 \times 200$  for point-wise calculations of the potential.

FIG. 1

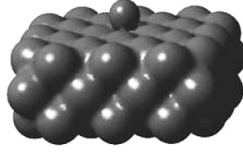


Our adsorbed surface model employed in our calculations. The sphere on the top represents the adsorbed atom (H or Na) and the 72 other spheres correspond to Al atoms disposed in three layers, mimicking the Al(100) surface.

In order to implement our close-coupling calculations, the coordinate system is set so that the origin is located at the adsorbate, and the direction of the  $z$ -axis corresponds to the normal of the aluminum surface. A grid of  $73 \times 73 \times 102$  points is employed for  $x$ ,  $y$ ,  $z$  coordinates, respectively, each of which extends from  $-15$  to  $15$  atomic units. This grid size is found to be sufficient in order to obtain accurate data for the surface potential with the use of a triple linear interpolation scheme.

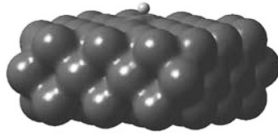
Isovalued surface of the electron density of the [H-Al(100)]<sup>+</sup> system with an isovalue of 0.01 is shown in Fig. 2, while that of the [Na-Al(100)]<sup>+</sup> system is presented in Fig. 3. We can notice a conspicuous difference between these two systems, that is, for the [H-Al(100)]<sup>+</sup> system, the electron density distribution concentrates in the vicinity of the adsorbed H atom, while it disperses into the aluminum surface for the [Na-Al(100)]<sup>+</sup> system. This is due to the fact that the Pauling electron affinity value of H atom, 2.1, is larger than that of Al atom, 1.5, and that of Al atom is larger than that of Na atom, 0.9. From this observation, we can expect

FIG. 2



Isovalued surface of the electron density of the  $[\text{H-Al}(100)]^+$  system with an isovalue of 0.01.

FIG. 3



Isovalued surface of the electron density of the  $[\text{Na-Al}(100)]^+$  system with an isovalue of 0.01.

that charge-transfer process with the  $\text{H}^+$  ions can occur more easily with the  $[\text{H-Al}(100)]$  system than for the  $[\text{Na-Al}(100)]$  system.

The above obtained electrostatic potential  $V_e$  allows us to calculate the electronic wave functions of the adsorbed surface. The Hamiltonian, including the electrostatic potential, is represented in a set of orthonormalized Sturmian-type basis functions [7]. A diagonalization of the Hamiltonian matrix yields the surface electronic wave functions  $\psi_i^s$  and eigenenergies  $\varepsilon_i^s$ . Unfortunately, only the ground state wave function is meaningful among those calculated in the present treatment. In practice, we therefore include only the ground state wave function  $\psi_0^s$  into our close-coupling calculations.

## 2. Dynamics

Collision dynamics between the  $\text{H}^+$  ion and an atom adsorbed on the aluminum surface is studied using a close-coupling approach within the semiclassical representation [7-9]. We first designate  $\vec{R}=(R_x, R_y, R_z)$  as the position of the ion and  $\vec{r}=(x, y, z)$  as that of the electron. The motion of the projectile ( $\text{H}^+$  ion) is treated classically and that of the electron is described quantum-mechanically. The  $\text{H}^+$  ion moves in the potential  $-V_e$ , but it is also affected by the response of the surface to the projectile. This can be approximated (principally in the limit of small projectile velocity or enough large distances) by the classical concept of “image charge” (see for example [10]), and expressed as the interaction between the  $\text{H}^+$  ion and the classical image of the projectile

$$V_p(R_z) \approx -\frac{1}{4d}, \quad (1)$$

where  $d$  denotes the distance between the ion and the classical image plane  $z_{im}$ . The classical image plane is located at a (positive) distance of  $z_{im} = z_{jellium} + \Delta z_{im} = z_{jellium} + 1.25 - 0.2r_s$  from the topmost Al atomic layer.  $z_{jellium}$  is defined as half a lattice spacing of the Al surface, and we have a Wigner-Seitz radius of  $r_s = 2.07$  a.u. for the aluminum metal surface.

The motion of the electron is governed by the surface potential  $V_e$ , the Coulomb potential of the H<sup>+</sup> ion  $V_H$ , and the interaction  $V_{pe}$  between the electron and the classical image of the projectile.  $V_e$  corresponds to the electrostatic potential of the adsorbed surface, as described previously. The Coulomb potential is given by  $V_H(\vec{R}, \vec{r}) = -1/r_H$ , where  $\vec{r}_H$  is the electron coordinate measured from the H<sup>+</sup> ion. The interaction between the electron and the classical image of the projectile is given by

$$V_{pe}(\vec{R}, \vec{r}) \approx \frac{1}{D}, \quad (2)$$

where  $D$  is the electron distance from the image of the projectile. This expression corresponds to the case where the electron is outside the Al surface. On the surface,  $V_H(\vec{R}, \vec{r})$  and  $V_{pe}(\vec{R}, \vec{r})$  cancel each other and vanish inside the Al surface.

The equation of motion for the H<sup>+</sup> ion can be written as

$$m_p \frac{d^2 \vec{R}}{dt^2} = -\vec{\nabla}_R [-V_e(\vec{R}) + V_p(R_z)], \quad (3)$$

where  $m_p$  denotes the proton mass. The Hamiltonian for an electron in the presence of the H<sup>+</sup> ion and the adsorbed surface is expressed in atomic units as

$$H(\vec{R}, \vec{r}) = -\frac{1}{2} \nabla_r^2 + V_H(\vec{R}, \vec{r}) + V_e(\vec{r}) + V_{pe}(\vec{R}, \vec{r}). \quad (4)$$

In the close-coupling description of ion-surface collisions, the motion of the electron is constrained to a configuration space which is given by a finite set of basis functions. We approximate the time-dependent electronic wave function by the expansion

$$\Psi(\vec{r}, t) = c_0^s(t) \psi_0^s(\vec{r}) + \sum_j c_j^H(t) \psi_j^H(\vec{r}_H) \exp[i\vec{R} \cdot \vec{r}]. \quad (5)$$

Here,  $\psi_0^s(\vec{r})$  represents the ground-state electronic wave function of the adsorbed surface and  $c_0^s(t)$  the time-dependent complex amplitude for the occupation of this state, corresponding to the initial state.  $\psi_j^H(\vec{r}_H)$  denotes the eigen wave functions of an electron in the Coulomb potential of the H<sup>+</sup> ion, corresponding to the hydrogen quantum numbers  $j \equiv (nlm)$  and associated to the eigenenergies  $\varepsilon_{nlm} = -1/2n^2$ , and  $c_j^H(t)$  the time-dependent complex amplitude for the occupation of these states. The factor  $\exp[i\vec{R} \cdot \vec{r}]$  is the electron translation factor (ETF), and represents an additional linear momentum carried away by the electron captured by the moving H<sup>+</sup> ion at infinite separations.

The amplitudes  $c_0^s(t)$  and  $c_j^H(t)$  can be calculated by requiring the wave function in Eq. (5) to obey the time-dependent Schrödinger equation:

$$i\frac{\partial}{\partial t}\Psi(\vec{r}, t) = H(\vec{R}, \vec{r})\Psi(\vec{r}, t). \quad (6)$$

Insertion of the expansion (5) leads to a set of coupled equations for  $c_0^s(t)$  and  $c_j^H(t)$ :

$$\begin{aligned} i\dot{c}_0^s + i\sum_j \dot{c}_j^H \left\langle \psi_0^s \left| e^{i\vec{R}\cdot\vec{r}} \right| \psi_j^H \right\rangle &= c_0^H \left[ \varepsilon_0^s - \left\langle \psi_0^s \left| \frac{1}{r_H} - V_{pe} \right| \psi_0^s \right\rangle \right] \\ &+ \sum_j c_j^H \left[ \left( \varepsilon_j^H + \frac{1}{2}\dot{R}^2 \right) \left\langle \psi_0^s \left| e^{i\vec{R}\cdot\vec{r}} \right| \psi_j^H \right\rangle + \left\langle \psi_0^s \left| e^{i\vec{R}\cdot\vec{r}} \left( V_e + \vec{R}\cdot\vec{r} \right) \right| \psi_j^H \right\rangle \right], \\ i\dot{c}_0^s \left\langle \psi_j^H \left| e^{-i\vec{R}\cdot\vec{r}} \right| \psi_0^s \right\rangle + i\dot{c}_j^H &= c_0^H \left[ \varepsilon_0^s \left\langle \psi_j^H \left| e^{-i\vec{R}\cdot\vec{r}} \right| \psi_0^s \right\rangle - \left\langle \psi_j^H \left| e^{-i\vec{R}\cdot\vec{r}} \left( \frac{1}{r_H} - V_{pe} \right) \right| \psi_0^s \right\rangle \right] \\ &+ c_j^H \left( \varepsilon_j^H + \frac{1}{2}\dot{R}^2 \right) + \sum_{j'} c_{j'}^H \left\langle \psi_j^H \left| \left( V_e + V_{pe} + \vec{R}\cdot\vec{r} \right) \right| \psi_{j'}^H \right\rangle. \end{aligned} \quad (7)$$

Supposing that the amplitudes have initial values

$$c_0^s(-\infty) = 1, \quad c_j^H(-\infty) = 0, \quad (8)$$

the transition probability for the electron to be found in state  $f$ , after the completion of the collision along a trajectory  $\vec{R}$  is then given by

$$P_{0 \rightarrow f}(+\infty) = |c_f^H(+\infty)|^2. \quad (9)$$

The transition amplitudes  $c_f^H(+\infty)$  can be related to measurable quantities like integrated partial cross sections and angle differential cross sections. Particularly, the total cross section is given by

$$\sigma_{0 \rightarrow f} = 2\pi \int_0^\infty db b P_{0 \rightarrow f}(+\infty), \quad (10)$$

and the total cross section for charge transfer by

$$\sigma_{total} = \sum_f \sigma_{0 \rightarrow f}, \quad (11)$$

where the summation is carried out over all the charge transfer states. Note also that, during the calculation, the conservation of probability is monitored so that

$$|c_0^s(t)|^2 + \sum_j |c_j^H(t)|^2 = 1. \quad (12)$$

The Runge-Kutta method is used in order to solve numerically Eqs. (7). The most time-consuming part of the calculation is the evaluation of the matrix elements in Eqs. (7), which are calculated using the spherical coordinates  $(r, \theta, \varphi)$  with 32 point Gauss-Laguerre, Gauss-Legendre, and equidistant quadratures, respectively. This part of the calculation is parallelized with MPI (message passing interface) library to run on a multiple-processor computer. Typically, one 500-time-step calculation with 6 channels needs about 5 minutes of elapsed time

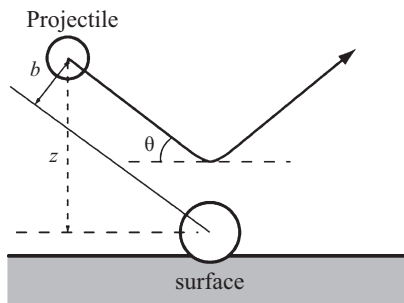
using 16 processors on a SGI Altix 4700 supercomputer.

### III. Results

#### 1. H-adsorbed Al(100)

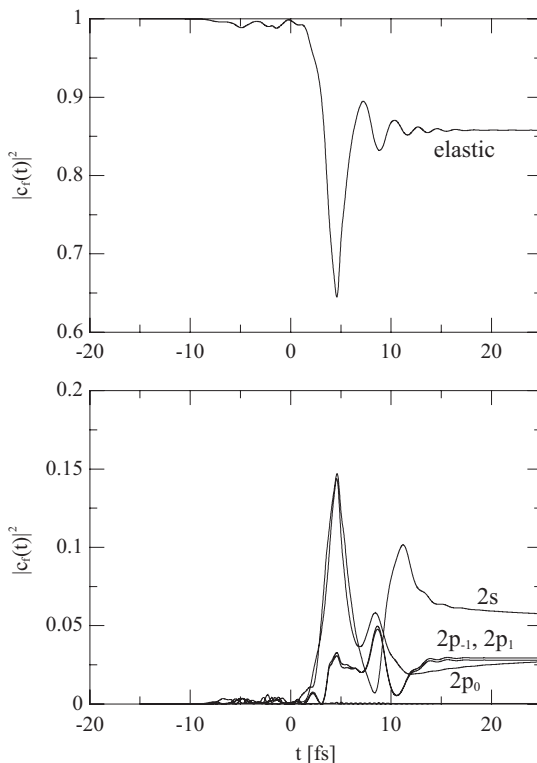
We first study the collision process between a H<sup>+</sup> ion (projectile) and a hydrogen atom (target) adsorbed on the Al(100) surface. We suppose that the motion of the projectile is confined within the  $xz$ -plane and the adsorbed surface is fixed in the configuration space. The projectile collides with the target at an incident angle of  $\theta=0.2^\circ$  with respect to the Al(100) surface plane, an impact parameter of  $b=0.05\text{a.u.}$  with respect to the target, with a kinetic energy of  $E_p=40\text{eV}$  (for the coordinate system used in the present study, see Fig. 4). The initial position of the projectile is set at a position that is enough far from the surface and where the potential from the adsorbed surface is negligible. The duration time for the calculation is also chosen so that the projectile at the end of the time evolution is enough far from the surface. In Fig. 5, we show the time evolution of the occupation probabilities  $|c_j^{s,H}(t)|^2$  of different states during the collision. The occupation probability  $|c^s(t)|^2$  of the ground electronic state of the H-adsorbed surface is presented at the top of Fig. 5, whereas those of  $1s$ ,  $2s$ ,  $2p_{-1}$ ,  $2p_0$ , and  $2p_1$  states of the H<sup>+</sup> ion,  $|c_{nm}^H(t)|^2$  are plotted at the bottom. The origin of the time  $t$  is chosen so that the H<sup>+</sup> ion be found at the closest position to the adsorbed hydrogen atom at  $t=0$ . We observed that these occupation probabilities change significantly mainly for  $t>0$ , that is, when the H<sup>+</sup> goes away from the adsorbed atom. Those for large, positive  $t$  (after the collision) correspond to the probabilities for elastic scattering or charge transfer. In the present case, the electron is found to be mostly in the electronic ground state of the H-adsorbed surface, or in other words the elastic scattering is the dominant process. Charge transfer into  $2s$  state is found to be the next dominant process. We found that the probabilities for charge transfer to  $2p_{+1}$  and  $2p_{-1}$  take indistinguishably equal values from each other. The probabilities for charge transfer to  $2p_0$  and  $2p_{\pm 1}$  states are found to be comparable in

FIG. 4



Coordinate system for collisions between an ion and an adsorbed atom

FIG. 5

 $E_p=40$  eV,  $\theta=0.2$  deg.

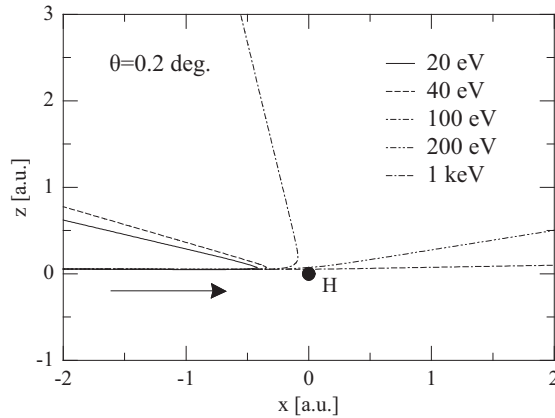
Time-dependence of the probabilities for the electron to be found in the ground state of the [H-Al(100)] surface (elastic scattering), to be captured in  $1s$ ,  $2s$ ,  $2p_{-1}$ ,  $2p_0$  and  $2p_1$  states by the  $H^+$  ion after the collision. The incident angle is  $\theta=0.2^\circ$  with respect to the aluminum surface plane, the impact parameter is  $b=0.05$  a.u. with respect to the adsorbate, and the initial kinetic energy of the  $H^+$  ion is  $E_p=40$  eV.

magnitude. The probability for charge transfer to  $1s$  state is invisibly small, so that this process is almost negligible.

The trajectory of the  $H^+$  ion for  $\theta=0.2^\circ$ ,  $b=0.05$  a.u., and  $E_p=40$  eV is shown in Fig. 6, together with those for  $E_p=20, 100, 200$ , and  $1000$  eV with the same incident angle  $\theta$  and impact parameter  $b$ . Obviously, the larger the incident kinetic energy is, the smaller the deflection angle becomes. In the limit of large energies  $E_p \rightarrow \infty$ , the proton trajectory approaches a straight line.

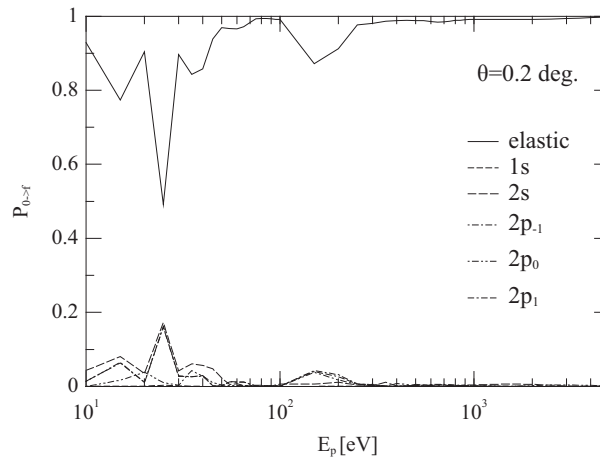
In Fig. 7, the transition probabilities  $P_{0 \rightarrow j}(+\infty)$  are plotted as functions of the initial kinetic energy of the  $H^+$  ion and for a fixed incident angle of  $\theta=0.2^\circ$ . The probabilities are found to oscillate as function of the energy for smaller values, that is,  $E_p < 200$  eV. For this energy range, the elastic scattering process is by far dominant and the probability takes its

FIG. 6



Trajectories of the H<sup>+</sup> ion in the potential of [H-Al(100)] for initial kinetic energies of 20, 40, 100, 200 and 1000 eV and a fixed incident angle of  $\theta=0.2^\circ$ .

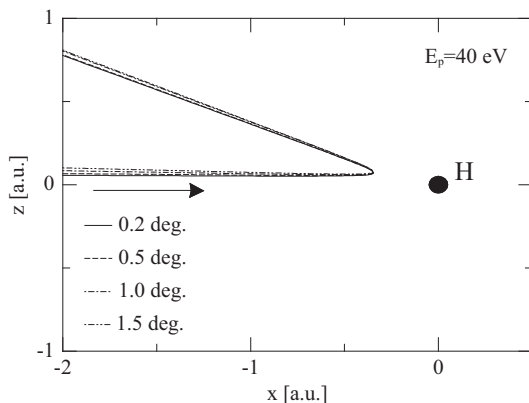
FIG. 7



Energy-dependence of the probabilities for the electron to be found in the ground state of the [H-Al(100)] surface (elastic scattering), to be captured in 1s, 2s, 2p<sub>-1</sub>, 2p<sub>0</sub> and 2p<sub>1</sub> states by the H<sup>+</sup> ion after the collision. The incident angle is fixed to the value of  $\theta=0.2^\circ$ .

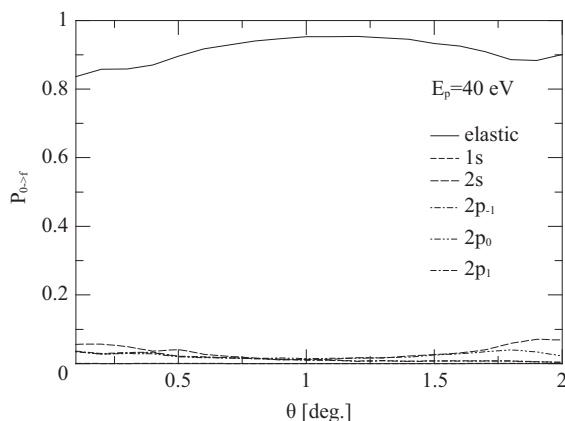
minimum value of about 50%, for a kinetic energy of about 25 eV. The other transition probabilities take roughly similar values in magnitude except for that to 1s state. Particularly, the probabilities for charge transfer to 2p<sub>0</sub> and 2p<sub>±1</sub> states take their maximum value of about

FIG. 8



Trajectories of the  $H^+$  ion in the potential of  $[H-Al(100)]^+$  for incident angles of  $0.2^\circ$ ,  $0.5^\circ$ ,  $1.0^\circ$  and  $1.5^\circ$ , and a fixed initial kinetic energy of  $E_p=40$ eV.

FIG. 9



Angle-dependence of the probabilities for the electron to be found in the ground state of the  $[H-Al(100)]$  surface (elastic scattering), to be captured in  $1s$ ,  $2s$ ,  $2p_{-1}$ ,  $2p_0$  and  $2p_1$  states by the  $H^+$  ion after the collision. The initial kinetic energy is fixed to  $E_p=40$ eV.

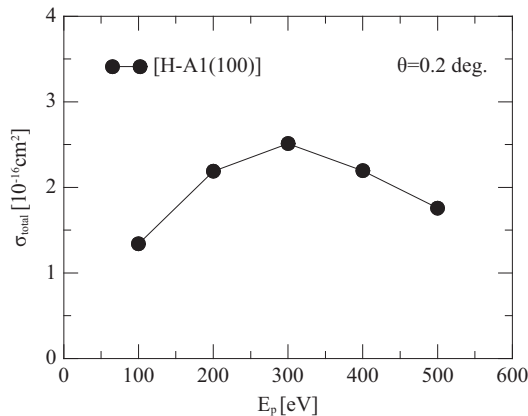
17%. The behavior of the probabilities is rather smooth for higher energies, that is,  $E_p > 200$ eV. As the initial kinetic energy of the  $H^+$  ion increases, the probability for elastic scattering approaches 100% and those for charge transfer to different states tend to 0%.

Next, we fix the initial kinetic energy of the  $H^+$  ion with a value of  $E_p=40$ eV and change the incident angle  $\theta$ . The trajectories of the  $H^+$  ion are shown in Fig. 8 for incident angles of  $0.2^\circ$ ,  $0.5^\circ$ ,  $1.0^\circ$ , and  $1.5^\circ$ . Here, the deflection angle is found to be invariant as a function of the

incident angle with a fixed value of the initial kinetic energy of the H<sup>+</sup> ion. In Fig. 9, the transition probabilities are plotted as functions of the incident angle for a fixed initial kinetic energy of  $E_p=40$  eV. They do not show any change as functions of the angle, so that their angle dependence is rather weak. The probability for elastic scattering takes values roughly between 85 and 95%, the others between 0 and 10%. But, again the transition probability to 1s state is negligible.

Finally, in Fig. 10, we show the total integrated cross section  $\sigma_{total}$  for charge transfer in collisions between the H<sup>+</sup> ion and the [H-Al(100)] surface as a function of the incident kinetic energy of the H<sup>+</sup> ion. The cross section is found to take values between  $1 \times 10^{-16}$  and  $3 \times 10^{-16}$  cm<sup>2</sup> between 100 and 500 eV. It reaches its maximum value for about 300 eV.

FIG. 10

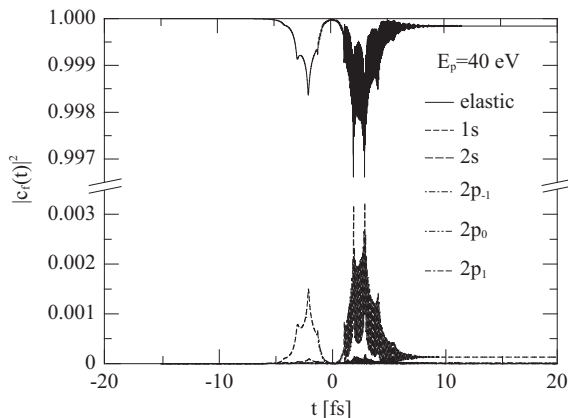


Total cross section for charge transfer in collisions between the H<sup>+</sup> ion and the [H-Al(100)] surface as a function of the incident kinetic energy. The incident angle of the H<sup>+</sup> ion with respect to the aluminum surface is  $\theta=0.2^\circ$ .

## 2. Na-adsorbed Al(100)

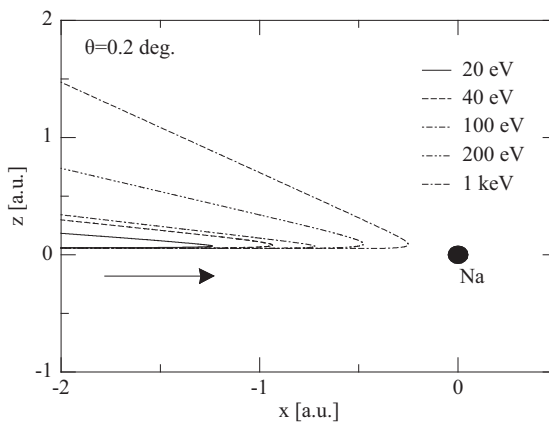
Next, we consider the collision process between a H<sup>+</sup> ion and a Na atom adsorbed on the Al(100) surface. As in the case of the adsorbed hydrogen atom, we consider the H<sup>+</sup> ion moving within the  $xz$ -plane, at an incident angle of  $\theta=0.2^\circ$ , an impact parameter of  $b=0.05$  a.u. The initial kinetic energy of the H<sup>+</sup> ion is  $E_p=40$  eV. The time evolution of the occupation probabilities  $|c_j^H(t)|^2$  of different states is shown in Fig. 11 (a care should be taken of the scale of the probability). The H<sup>+</sup> ion is found to be at the closest position to the Na atom at  $t=0$ . We observed that they do not show any change during the time evolution: the occupation probability  $|c_0^H(t)|^2$  of the surface ground electronic state varies between 99.7% and 100%, while those corresponding to charge transfer to different states  $|c_{nim}^H(t)|^2$  are negligibly small, and found to take values less than 0.2%. In contrast to the [H-Al(100)] surface, in other words, we

FIG. 11



Time-dependence of the probabilities for the electron to be found in the ground state of the [Na-Al(100)] surface (elastic scattering), to be captured in  $1s$ ,  $2s$ ,  $2p_{-1}$ ,  $2p_0$  and  $2p_1$  states by the  $H^+$  ion. The incident angle is  $\theta=0.2^\circ$  with respect to the aluminum surface plane, the impact parameter is  $b=0.05a.u.$  with respect to the adsorbate, and the initial kinetic energy of the  $H^+$  ion is  $E_p=40eV$ .

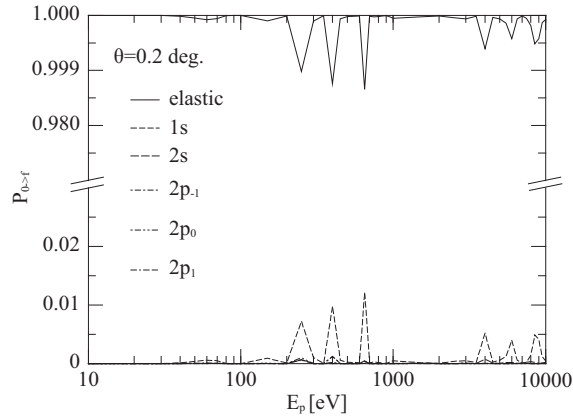
FIG. 12



Trajectories of the  $H^+$  ion in the potential of  $[Na-Al(100)]^+$  for initial kinetic energies of 20, 40, 100, 200 and 1000 eV and a fixed incident angle of  $\theta=0.2^\circ$ .

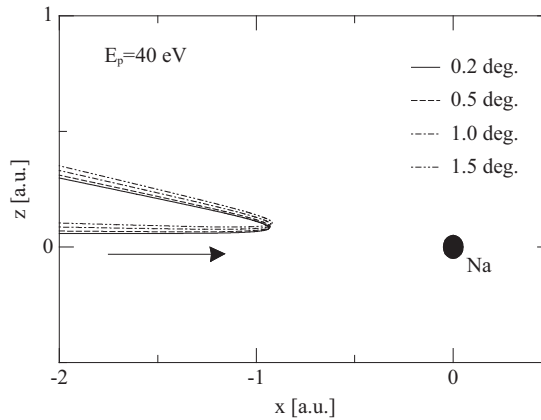
observe the elastic scattering for almost 100% of probability and the charge transfer for almost 0%. We observe that the charge transfer process from the [Na-Al(100)] surface to the  $H^+$  is almost negligible in this case.

FIG. 13



Energy dependence of the probabilities for the electron to be found in the ground state of the [Na-Al(100)] surface (elastic scattering), to be captured in  $1s$ ,  $2s$ ,  $2p_{-1}$ ,  $2p_0$  and  $2p_1$  states by the  $H^+$  ion after the collision. The incident angle is fixed to the value of  $\theta=0.2^\circ$ .

FIG. 14



Trajectories of the  $H^+$  ion in the potential of  $[Na-Al(100)]^+$  for incident angles of  $0.2^\circ$ ,  $0.5^\circ$ ,  $1.0^\circ$  and  $1.5^\circ$ , and a fixed initial kinetic energy of  $E_p=40\text{eV}$ .

The trajectory of the  $H^+$  ion for  $\theta=0.2^\circ$ ,  $b=0.05\text{a.u.}$ , and  $E_p=40\text{eV}$  is shown in Fig. 12, together with those for  $E_p=20, 100, 200$ , and  $1000\text{ eV}$  with the same incident angle and impact parameter. As in the case of the H-adsorbed surface, the higher the initial kinetic energy is, the smaller the deflection angle is. With the increasing initial kinetic energy, the  $H^+$  ion approaches closer to the adsorbed atom. For a given initial kinetic energy, the deflection angle is much

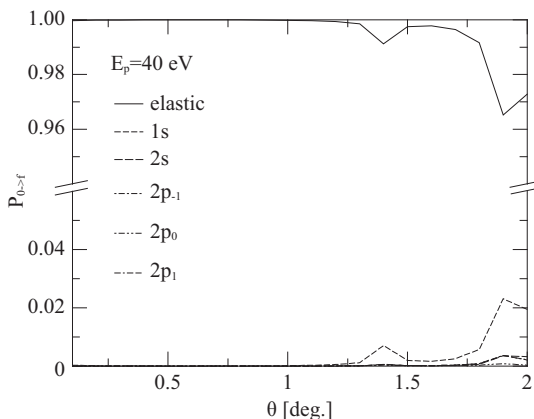
larger than in the case of the H-adsorbed surface. This is due to the fact that the repulsion of H atom is stronger than that of Na atom.

The energy dependence of the transition probabilities  $P_{0 \rightarrow f}(+\infty)$  for a fixed incident angle  $\theta=0.2^\circ$  is shown in Fig. 13. For all energies between 10 eV and 10 keV, the elastic scattering is by far the dominant process and its transition probability varies between 98.5% and 100%. The probabilities for electron capture in  $2s$ ,  $2p_{-1}$ ,  $2p_0$  and  $2p_{+1}$  are negligible, while that in  $1s$  state oscillates for  $E_p > 100\text{eV}$  between the values of 0% and 1.5%.

We next fix the initial kinetic energy of the  $\text{H}^+$  ion with the value of  $E_p=40\text{eV}$  and change the incident angle  $\theta$ . The trajectories of the  $\text{H}^+$  ion are shown in Fig. 14 for incident angles of  $0.2^\circ$ ,  $0.5^\circ$ ,  $1.0^\circ$  and  $1.5^\circ$ . As in the case of the  $[\text{H-Al}(100)]$  surface, the deflection angle appears to be invariant with changes of the incident angle  $\theta$ , given a fixed value of the initial kinetic energy  $E_p$  of the  $\text{H}^+$  ion.

In Fig. 15, the transition probabilities  $P_{0 \rightarrow f}(+\infty)$  are plotted as functions of the incident angle  $\theta$  for a fixed initial kinetic energy of  $E_p=500\text{eV}$ . It is always observed that elastic scattering is by far the dominant process and the charge transfer probabilities are generally very small except for that to  $1s$  charge-transfer state, which reaches a value of about 2% at about  $\theta=2^\circ$ .

FIG. 15

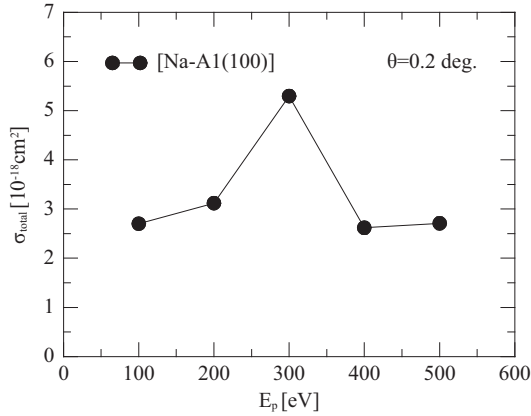


Angle dependence of the probabilities for the electron to be found in the ground state of the  $[\text{Na-Al}(100)]$  surface (elastic scattering), to be captured in  $1s$ ,  $2s$ ,  $2p_{-1}$ ,  $2p_0$  and  $2p_1$  states by the  $\text{H}^+$  ion after the collision. The initial kinetic energy is fixed to  $E_p=40\text{eV}$ .

In Fig. 16, we show the total cross section for charge transfer in collisions between the  $\text{H}^+$  ion and the  $[\text{Na-Al}(100)]$  surface as a function of the incident kinetic energy. As expected, it is found to take very small values (almost two orders of magnitude) compared with that in the case of the  $[\text{H-Al}(100)]$  surface. The cross section takes values of some of  $10^{-18}\text{cm}^2$ .

So far, we have observed that charge-transfer process is significant for the  $[\text{H-Al}(100)]$  system, but it is negligible for the  $[\text{Na-Al}(100)]$  system. As mentioned above, the reason for this difference is due to the fact that the electron charge distribution is localized in the vicinity

FIG. 16



Total cross section for charge transfer in collisions between the H<sup>+</sup> ion and the [Na-Al(100)] surface as a function of the incident kinetic energy. The incident angle of the H<sup>+</sup> ion with respect to the aluminum surface is  $\theta=0.2^\circ$ .

of H atom in the [H-Al(100)] system, while it disperses into the aluminum surface in the [Na-Al(100)] system.

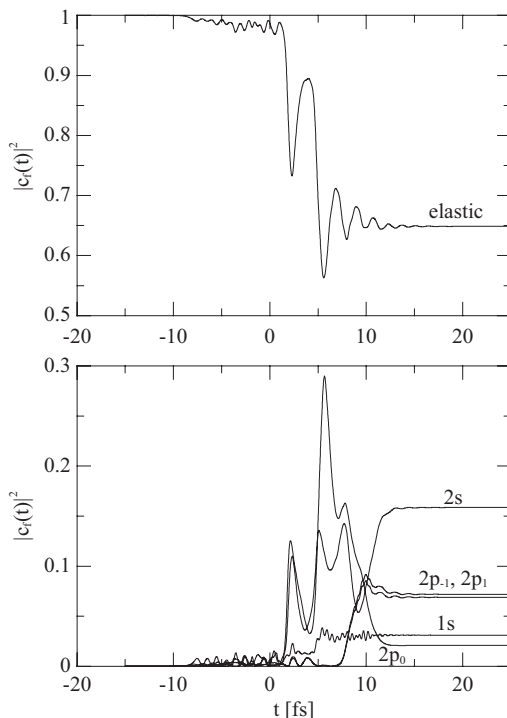
### 3. Effect of the Inclusion of the Dielectric Response

In the above calculations, we have taken into account of the dielectric response of the surface in the presence of the projectile (H<sup>+</sup> ion). Its exact effects onto the electron and the projectile are unknown, but we have approximated them in the form of the interactions between the electron and the image charge in Eq. (1), and between the projectile and the image charge in Eq. (2). Our aim here is to assess the effect of the inclusion of the potentials in Eqs. (1) and (2). To this end, we have also carried out calculations without these potentials.

Figure 17 presents the time evolution of the occupation probabilities  $|c_f^s{}^H(t)|^2$  of different states during the collision between the H<sup>+</sup> ion and the [H-Al(100)] surface. These are calculated as the same initial conditions  $\theta=0.2^\circ$ ,  $b=0.05\text{a.u.}$ , and  $E_p=40\text{eV}$  as those in Fig. 5, but without including the potentials in Eq. (1) and (2). We find that the elastic scattering is still the dominant process, but its probability after the collision is a little smaller than that in Fig. 5 including the potentials (1) and (2). In a similar way, the charge transfer to  $2s$  state is the next dominant process, but its probability is larger than that in Fig. 5. The remarkable difference is that the probability for charge transfer to  $1s$  is fairly large without inclusion of the potentials, while it is negligible with inclusion of them. The probability for charge transfer to  $2p_0$  state is found to be the smallest of those for all the processes.

Figure 18 shows the same results in the case of the [Na-Al(100)] surface, without including the potentials in Eqs. (1) and (2), to be compared with those in Fig. 11, which includes them. Comparing the results in Figs. 11 and 18, no remarkable qualitative difference is

FIG. 17

 $E_p=40$  eV,  $\theta=0.2$  deg.

Same results as in Fig. 5, but calculated without taking into account the potentials in Eqs. (1) and (2), which are due to the dielectric response of the surface.

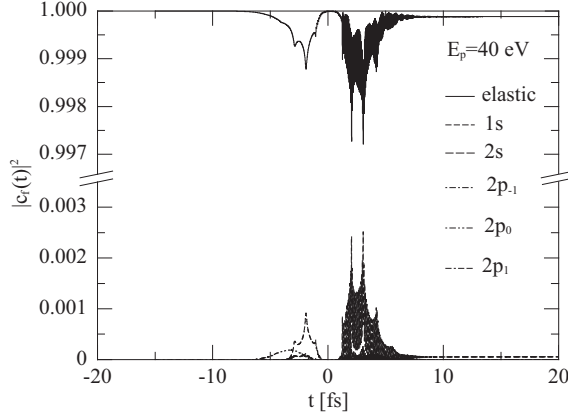
observed. We obtain almost a probability of almost 100% for elastic scattering and 0% for charge transfer, although the occupation probability of  $1s$  state reaches a value of about 0.3% during the collision.

#### 4. Alignment and Orientation of 2p Excited States

In previous sections, we have observed large charge-transfer probabilities between  $H^+$  ion and [H-Al(100)] surface, while almost only elastic scattering occurs between  $H^+$  ion and [Na-Al(100)] surface. In particular, we have found non-negligible probabilities for the electron to be captured in different 2p states in  $H^+ + [H-Al(100)]$  collisions. Therefore, it is interesting here to examine properties of those states. In this section, we shall study the orientation and alignment of 2p states in collisions between  $H^+$  ion and [H-Al(100)] surface.

The alignment and orientation of an excited atomic state are characterized by two parameters, namely the alignment angle  $\gamma$  and angular momentum  $\langle L_y \rangle$  [11, 12, 13]. The alignment angle is defined as the angle between the major axis of the electron cloud on the

FIG. 18



Same results as in Fig. 11, but calculated without taking into account the potentials in Eqs. (1) and (2), which are due to the dielectric response of the surface.

collision plane with respect to the incident direction of the projectile, while the orientation parameter describes the rotation of the electronic cloud. In our case, these parameters of  $2p$  excited states are defined by

$$\tan(2\theta - 2\gamma) = \frac{2[\lambda(1-\lambda)]^{1/2}}{1-2\lambda} \cos \chi, \quad (13)$$

$$\langle L_y \rangle = -2[\lambda(1-\lambda)]^{1/2} \sin \chi, \quad (14)$$

where  $\theta$  is the angle between the incident direction of the H<sup>+</sup> ion and the aluminum surface plane. The parameters  $\theta$  and  $\gamma$  are given by

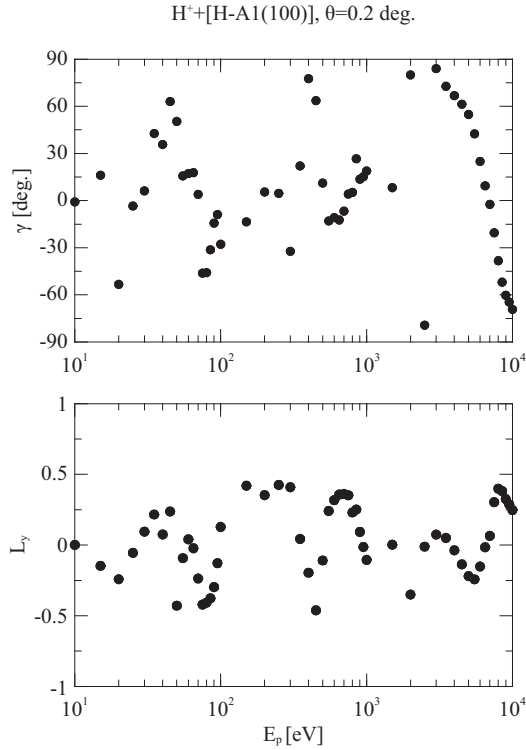
$$\lambda = \frac{|c_{2p_0}^H|^2}{(|c_{2p_0}^H|^2 + |c_{2p_1}^H|^2)}, \quad (15)$$

$$\chi = \arg(c_{2p_1}^H / c_{2p_0}^H), \quad (16)$$

In other words,  $\lambda$  gives the fractional probability for excitation to  $2p_0$  state, while  $\chi$  gives the relative phase between the  $2p_1$  and  $2p_0$  amplitudes.

In Figs. 19, the alignment angle  $\gamma$  and angular momentum  $\langle L_y \rangle$  are plotted as functions of the incident kinetic energy  $E_p$ , for a fixed incident angle of  $\theta = 0.2^\circ$ . The behavior of the alignment angle  $\gamma$  with changes of the incident kinetic energy is very complicated and it is difficult to make even qualitative description. However, it is observed that for large values of  $E_p$ ,  $\gamma$  decreases with increasing energy. The dependence of the angular momentum  $\langle L_y \rangle$  on  $E_p$  is similarly complicated and it shows small oscillations as a function of the energy  $E_p$  between the values of  $-0.5$  and  $0.5$ . In Figs. 20, we show the alignment angle  $\gamma$  and the angular momentum  $\langle L_y \rangle$  as function of the incident angle  $\theta$ . The alignment angle increases smoothly and slowly with increasing incident angle. The angular momentum  $\langle L_y \rangle$  also does not change

FIG. 19



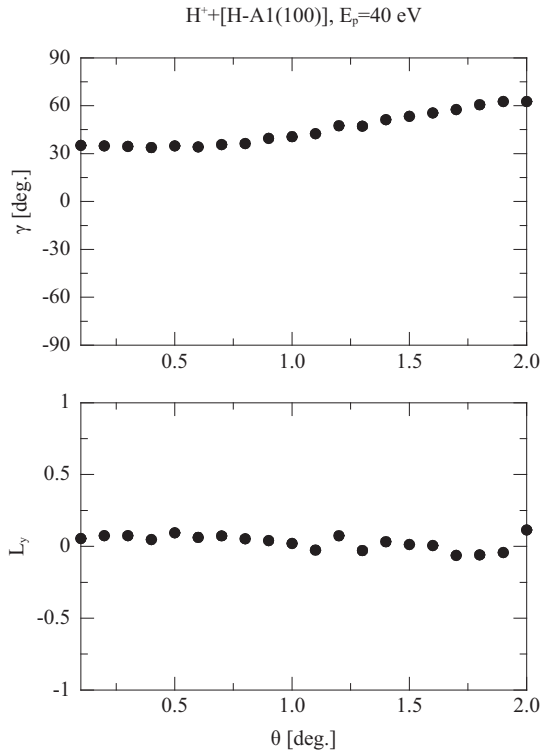
Alignment angle  $\gamma$  (above) and angular momentum  $\langle L_y \rangle$  as functions of the initial kinetic energy  $E_p$  in collisions between the  $H^+$  ion and the  $[H-Al(100)]$  surface. The incident angle is fixed to  $\theta=0.2^\circ$ .

significantly as a function of  $\theta$ , and takes values between  $-0.2$  and  $+0.2$ .

#### IV. Summary

In this work, we have studied charge-transfer process in collisions between a  $H^+$  atom and an atom-adsorbed surface, using a semiclassical close-coupling approach. Charge transfer is found to be important for the  $[H-Al(100)]$  system, while almost only elastic scattering occurs for the  $[Na-Al(100)]$ . This is due to the difference in the electron charge distribution between these two systems. As an extension of this work, it is interesting to study excitation and ionization of the adsorbed surface by  $H^+$ -ion impact.

FIG. 20



The alignment angle  $\gamma$  (above) and angular momentum  $\langle L_y \rangle$  as functions of the incident angle  $\theta$  in collisions between the H<sup>+</sup> ion and the [H-Al(100)] surface. The initial kinetic energy is fixed to  $E_p = 40\text{eV}$ .

### REFERENCES

- [ 1 ] D.C. Langreth and P. Nordlander, Phys. Rev. B **43**, 2541 (1991).
- [ 2 ] H. Shao, D.C. Langreth, and P. Nordlander, Phys. Rev. B **49**, 13929 (1994).
- [ 3 ] H. Shao, P. Nordlander, and D.C. Langreth, Phys. Rev. B **52**, 2988 (1995).
- [ 4 ] W. Hübner and L.M. Falicov, Phys. Rev. B **47**, 8783 (1993).
- [ 5 ] H. Winter, Phys. Rep. **367**, 387 (2002).
- [ 6 ] Gaussian 98, Revision A.11.2, M. J. Frisch, G. W. Trucks, H. B. Schlegel, G. E. Scuseria, M. A. Robb, J. R. Cheeseman, V. G. Zakrzewski, J. A. Montgomery, Jr., R. E. Stratmann, J. C. Burant, S. Dapprich, J. M. Millam, A. D. Daniels, K. N. Kudin, M. C. Strain, O. Farkas, J. Tomasi, V. Barone, M. Cossi, R. Cammi, B. Mennucci, C. Pomelli, C. Adamo, S. Clifford, J. Ochterski, G. A. Petersson, P. Y. Ayala, Q. Cui, K. Morokuma, N. Rega, P. Salvador, J. J. Dannenberg, D. K. Malick, A. D. Rabuck, K. Raghavachari, J. B.

Foresman, J. Cioslowski, J. V. Ortiz, A. G. Baboul, B. B. Stefanov, G. Liu, A. Liashenko, P. Piskorz, I. Komaromi, R. Gomperts, R. L. Martin, D. J. Fox, T. Keith, M. A. Al-Laham, C. Y. Peng, A. Nanayakkara, M. Challacombe, P. M. W. Gill, B. Johnson, W. Chen, M. W. Wong, J. L. Andres, C. Gonzalez, M. Head-Gordon, E. S. Replogle, and J. A. Pople, Gaussian, Inc., Pittsburgh PA, (2001).

[ 7 ] W. Fritsch and C.D. Lin, Phys. Rep. **202**, 1 (1991).

[ 8 ] M. Kimura and N.F. Lane, Adv. At., Mol. Opt. Phys. **26**, 79 (1989).

[ 9 ] B. Pons, Phys. Rev. Lett. **84**, 4569 (2000).

[10] J.D. Jackson, Classical Electrodynamics, 2<sup>nd</sup> Edition, Wiley, New York (1975).

[11] M. Kimura and N.F. Lane, Phys. Rev. Lett. **56**, 2160 (1986).

[12] N. Andersen, J.W. Gallagher, and I.V. Hertel, Phys. Rep. **165**, 1 (1988).

[13] C.D. Lin, R. Shingal, A. Jain, and W. Fritsch, Phys. Rev. A **39** 4455 (1989).